# Syntheses, crystal structures and optical spectroscopy of $Ln_2(SO_4)_3 \cdot 8H_2O$ ($Ln$=Ho, Tm) and $Pr_2(SO_4)_3 \cdot 4H_2O$

Karolina Kazmierczak, Henning A. Höppe *

*Institut für Physik, Universität Augsburg, Universitätsstraße 1, D-86159 Augsburg, Germany*

## 1. Introduction

Rare-earth sulphates and their hydrates show a rich crystal chemistry due to the structural influence of crystal water molecules forming more or less complicated hydrogen bonded networks. With increasing crystal water content tetrahydrates $M_2(SO_4)_3 \cdot 4H_2O$ ($M$=La, Nd [1], Ce [2], Er [3]) and even octahydrates $M_2(SO_4)_3 \cdot 8H_2O$ ($M$=Y [4], Ce [5], Pr [6], Nd [7], Sm [8], Eu [9], Gd [10], Tb [3], Dy [5], Er [11], Yb [12], Lu [5]) are formed. These sulphates crystallise isotypically in space group $C2/c$. Such rare-earth sulphates may also act as catalysts in the chemoselective oxidation of organic sulphides mediated by hydrogen peroxide [13].

Quite frequently, a detailed single-crystal structure analysis reveals structural details which probably would have been overseen by just comparing X-ray powder patterns of presumably isotypic compounds. For example we recently presented an investigation on the mixed sulphate mono-hydrates $KLn(SO_4)_2 \cdot H_2O$ ($Ln$=La, Nd, Sm, Eu, Gd, Dy) [14] where we identified an unprecedented change in the lanthanoids' coordination by a slight rotation of a sulphate anion.

Moreover, the crystallisation of rare-earth sulphates is still not straightforward. In contrast to phosphates or silicates these cannot be prepared by high-temperature syntheses due to rather low decomposition temperatures. Therefore, crystals may only be obtained by crystallisation from solution in weeks or even months as in this contribution.

Herein we present the crystal structures, vibrational and optical spectra of the remaining two octahydrates $Ln_2(SO_4)_3 \cdot 8H_2O$ ($Ln$=Ho, Tm) and the tetrahydrate $Pr_2(SO_4)_3 \cdot 4H_2O$. We will finally compare the hydrogen bond networks of both structure types.

## 2. Experimental section

**Syntheses of $Ln_2(SO_4)_3 \cdot 8H_2O$ ($Ln$=Ho, Tm)**: Crystals of holmium and thulium sulphate octahydrate were obtained at room temperature by dissolving the respective lanthanide oxide ($Ho_2O_3/Tm_2O_3$, Auer, 99.99%) (75.6 mg/80.1 mg, 0.20 mmol) in 2 N $H_2SO_4$ (Merck, p.a, 96.0%) (10 ml, 0.020 mol). After slow evaporation at room temperature for several weeks non-hygroscopic pink single-crystals of $Ho_2(SO_4)_3 \cdot 8H_2O$ and colourless single-crystals of $Tm_2(SO_4)_3 \cdot 8H_2O$ could be obtained.

**Synthesis of $Pr_2(SO_4)_3 \cdot 4H_2O$**: Basically, $Pr_2(SO_4)_3 \cdot 4H_2O$ was synthesised analogously to $Ln_2(SO_4)_3 \cdot 8H_2O$ ($Ln$=Ho, Tm), but $Pr_2O_3$ (Auer, 99.9%) (45.4 mg, 0.100 mmol) could be dissolved in concentrated $H_2SO_4$ (Merck, p.a, 96.0%) (10 ml, 0.10 mol). Evaporation at room temperature for several months yielded green single-crystals.

The compositions of the obtained samples were checked by energy dispersive X-ray spectroscopy (EDX, $Ln$:P ratio) and the phase identification was carried out by powder X-ray diffraction.

**Crystal structure determination of $Ln_2(SO_4)_3 \cdot 8H_2O$ ($Ln$=Ho, Tm) and $Pr_2(SO_4)_3 \cdot 4H_2O$**: X-ray diffraction data were collected

* Corresponding author. Fax: +49 821 598 3032.
 *E-mail address:* henning@ak-hoeppe.de (H.A. Höppe).

on a Stoe IPDS 2 diffractometer (corrected numerically for absorption [15]) and on a Bruker AXS CCD diffractometer fitted with an APEX-II detector using Mo$K\alpha$ radiation at room temperature (corrected for absorption by applying a multi-scan correction [16]). The crystal structures of $Ln_2(SO_4)_3 \cdot 8H_2O$ ($Ln$=Ho, Tm) and $Pr_2(SO_4)_3 \cdot 4H_2O$ were solved by direct methods, using SHELXTL [17]. The relevant crystallographic data are summarised in Table 1. Tables 2–5 show the atomic coordinates and displacement parameters of $Ln_2(SO_4)_3 \cdot 8H_2O$ ($Ln$=Ho, Tm) and $Pr_2(SO_4)_3 \cdot 4H_2O$. Table 8 shows selected geometric parameters of $Ln_2(SO_4)_3 \cdot 8H_2O$ and $Pr_2(SO_4)_3 \cdot 4H_2O$. Tables 6 and 7 illustrate the hydrogen bonding geometry data.

Further details of the crystal structure investigations presented in this work may be obtained from the Fachinformationszentrum Karlsruhe, D-76344 Eggenstein-Leopoldshafen, Germany (e-mail: crysdata@fiz-karlsruhe.de) on quoting the depository numbers CSD-422432 ($Ho_2(SO_4)_3 \cdot 8H_2O$), CSD-422430 ($Tm_2(SO_4)_3 \cdot 8H_2O$) and CSD-422431 ($Pr_2(SO_4)_3 \cdot 4H_2O$), the names of the authors, and citation of this publication.

**Vibrational spectroscopy**: Infrared spectra were recorded at room temperature by using a Bruker IFS 66v/S spectrometer. The samples were thoroughly mixed with dried KBr (ca. 1 mg sample, 300 mg KBr). Raman spectra were recorded by a Bruker FRA 106/S module with a Nd–YAG laser ($\lambda$=1064 nm) with a scanning range from 400 to 4000 cm$^{-1}$.

**UV–vis spectroscopy**: The optical reflection spectra of samples of $Ho_2(SO_4)_3 \cdot 8H_2O$ and $Pr_2(SO_4)_3 \cdot 4H_2O$ were recorded using a UV–vis spectrophotometer Cary 300 Scan (Varian) and are shown in Figs. 6 and 7, respectively. The spectra were obtained from 200 to 800 nm applying a scan rate of 100 nm/min.

## 3. Crystal structure of $Ln_2(SO_4)_3 \cdot 8H_2O$ ($Ln$=Ho, Tm)

All octahydrates of the rare-earth sulphates crystallise in the monoclinic space group $C2/c$. The present structure determination of $Ho_2(SO_4)_3 \cdot 8H_2O$, as well as the investigation of $M_2(SO_4)_3 \cdot 8H_2O$ ($M$=Y [4], Ce [5], Pr [6], Nd [7], Sm [8], Eu [9], Gd [10], Tb, [3], Dy [5], Er [11], Yb [12], Lu [5]), prove that these compounds are centrosymmetric. The holmium cations form slightly undulated layers. Between the layers are voids in which sulphate tetrahedra and water molecules are located (Fig. 1). The Ho atoms are each square antiprismatically surrounded by eight oxygen atoms [HoO$_8$] (four of sulphate and four of crystal water molecules) with Ho–O distances of 2.281(4)–2.459(4) Å (Fig. 2). The two crystallographically inequivalent sulphate anions act as bidentate and tridentate ligands, respectively. The $\mu_2$-$SO_4^{2-}$ (S2) anions with S–O bond lengths of 1.456(4)–1.470(4) Å are linked to two Ho atoms and reside on two-fold rotation axes. The $\mu_3$-$SO_4^{2-}$ (S1) with S–O distances ranging from 1.450(4) to 1.491(4) Å are located in general positions.

The hydrogen bonds determined in $Ho_2(SO_4)_3 \cdot 8H_2O$ are shown in Table 6. All hydrogen atoms could be localised by difference Fourier syntheses and refined with fixed $U_{iso}$=0.02 Å$^2$. The hydrogen bonds with donator and acceptor distances between 2.73 and 3.04 Å can be classified as moderate according to the measures of Refs. [1,2]. The crystal water molecules

**Table 2**

Atomic coordinates, Wyckoff symbols and isotropic displacement parameters $U_{eq}$ (Å$^2$) for the atoms in $Ho_2(SO_4)_3 \cdot 8H_2O$.

| Atom | Wyckoff symbol | $x$ | $y$ | $z$ | $U_{eq}$ |
|------|------|------|------|------|------|
| Ho  | 8$f$ | 0.166272(17) | 0.47949(4) | 0.39202(2) | 0.0104(2) |
| S1  | 8$f$ | 0.21928(10)  | 0.52651(18) | 0.58920(8) | 0.0105(3) |
| O11 | 8$f$ | 0.1629(3)    | 0.5345(6)  | 0.6491(2)  | 0.0202(10) |
| O12 | 8$f$ | 0.1487(3)    | 0.5726(6)  | 0.5164(2)  | 0.0169(8) |
| O13 | 8$f$ | 0.3015(3)    | 0.6760(6)  | 0.6022(2)  | 0.0169(8) |
| O14 | 8$f$ | 0.2616(3)    | 0.3287(6)  | 0.5823(2)  | 0.0221(9) |
| S2  | 4$e$ | 0            | 0.1804(3)  | 0.2500     | 0.0115(4) |
| O21 | 8$f$ | 0.0842(3)    | 0.3056(6)  | 0.2874(2)  | 0.0227(9) |
| O22 | 8$f$ | 0.0343(3)    | 0.0550(6)  | 0.1935(2)  | 0.0201(9) |
| OW1 | 8$f$ | 0.3421(3)    | 0.5163(5)  | 0.4547(3)  | 0.0171(9) |
| OW2 | 8$f$ | 0.0408(3)    | 0.2681(6)  | 0.4364(2)  | 0.0175(9) |
| OW3 | 8$f$ | 0.2556(3)    | 0.5136(7)  | 0.2979(3)  | 0.0269(12) |
| OW4 | 8$f$ | 0.0168(3)    | 0.6634(6)  | 0.3605(3)  | 0.0308(11) |

**Table 1**

Crystal data and structure refinements.

|  | $Ho_2(SO_4)_3 \cdot 8H_2O$ | $Tm_2(SO_4)_3 \cdot 8H_2O$ | $Pr_2(SO_4)_3 \cdot 4H_2O$ |
|------|------|------|------|
| Temperature (K) | 298(2) | 298(2) | 298(2) |
| Molar weight (g/mol) | 762.17 | 770.17 | 642.06 |
| Crystal system | Monoclinic | Monoclinic | Monoclinic |
| Space group | $C2/c$ | $C2/c$ | $P2_1/n$ |
| $a$ (Å) | 13.4421(4) | 13.4118(14) | 13.051(3) |
| $b$ (Å) | 6.6745(2) | 6.6402(6) | 7.2047(14) |
| $c$ (Å) | 18.1642(5) | 18.1040(16) | 13.316(3) |
| $\beta$ (deg) | 102.006(1) | 101.980(8) | 92.55(3) |
| Cell volume (Å$^3$) | 1594.03(8) | 1577.2(3) | 1250.9(4) |
| $Z$ | 4 | 4 | 4 |
| Calculated density, $\rho_x$ (g cm$^{-3}$) | 3.176 | 3.244 | 3.409 |
| $\mu$ (mm$^{-1}$) | 10.353 | 11.681 | 8.289 |
| $F(000)$ | 1432 | 1448 | 1208 |
| Radiation | Mo$K\alpha$ radiation | Mo$K\alpha$ radiation | Mo$K\alpha$ radiation |
| Diffractometer | Bruker AXS CCD (APEX-II) | STOE IPDS 2 | STOE IPDS 2 |
| Absorption correction | Multi-Scan | Numerical | Numerical |
| Index range | 14/7/19 | 14/7/19 | 14/7/14 |
| Theta range ($\Theta_{min} - \Theta_{max}$) (deg) | 2.29–22.50 | 2.50–22.50 | 2.14–22.50 |
| Reflections collected | 8302 | 7166 | 5773 |
| Independent reflections | 1037 | 1023 | 1624 |
| $R_{int}$ | 0.051 | 0.087 | 0.082 |
| $R_1$ (all data) | 0.023 | 0.021 | 0.031 |
| w$R_2$ (all data) | 0.053 | 0.051 | 0.047 |
| Goodness of fit (GooF) | 1.184 | 1.182 | 0.856 |
| Residual electron density, min/max | −0.932/1.165 | −0.710/0.831 | −0.877/0.777 |

**Table 3**
Anisotropic displacement parameters $U_{ij}$ ($\text{Å}^2$) for the atoms in $Ho_2(SO_4)_3 \cdot 8H_2O$.

| Atom | $U_{11}$ | $U_{22}$ | $U_{33}$ | $U_{12}$ | $U_{13}$ | $U_{23}$ |
|---|---|---|---|---|---|---|
| Ho | 0.0105(3) | 0.0097(3) | 0.0110(2) | −0.00040(8) | 0.00221(14) | 0.00114(8) |
| S1 | 0.0106(7) | 0.0098(7) | 0.0113(7) | −0.0002(5) | 0.0026(6) | 0.0003(5) |
| O11 | 0.020(3) | 0.030(2) | 0.011(2) | −0.0016(16) | 0.0036(19) | −0.0028(16) |
| O12 | 0.0161(19) | 0.021(2) | 0.0131(19) | −0.0041(17) | 0.0012(15) | −0.0046(18) |
| O13 | 0.0145(18) | 0.012(2) | 0.023(2) | −0.0006(16) | 0.0011(15) | −0.0043(17) |
| O14 | 0.022(2) | 0.013(2) | 0.030(2) | −0.0006(17) | 0.0048(17) | 0.0005(17) |
| S2 | 0.0107(8) | 0.0133(10) | 0.0101(9) | 0 | 0.0012(7) | 0 |
| O21 | 0.0237(19) | 0.030(2) | 0.0140(19) | −0.0037(17) | 0.0031(15) | −0.0118(18) |
| O22 | 0.020(2) | 0.020(2) | 0.020(2) | −0.0046(18) | 0.0031(17) | 0.0010(18) |
| OW1 | 0.020(2) | 0.010(2) | 0.019(2) | 0.0001(14) | −0.0015(19) | −0.0007(16) |
| OW2 | 0.015(2) | 0.023(2) | 0.016(2) | −0.0092(17) | 0.0056(16) | −0.0041(17) |
| OW3 | 0.014(2) | 0.052(3) | 0.015(2) | −0.0082(19) | 0.004(2) | −0.0179(18) |
| OW4 | 0.0126(19) | 0.018(2) | 0.057(3) | 0.010(2) | −0.004(2) | 0.001(2) |

**Table 4**
Atomic coordinates, Wyckoff symbols and isotropic displacement parameters $U_{eq}$ ($\text{Å}^2$) for the atoms in $Pr_2(SO_4)_3 \cdot 4H_2O$.

| Atom | Wyckoff symbol | $x$ | $y$ | $z$ | $U_{eq}$ |
|---|---|---|---|---|---|
| Pr1 | 4e | 0.58577(4) | 0.24065(16) | 0.53548(4) | 0.0126(2) |
| Pr2 | 4e | 0.57368(5) | 0.23684(16) | 0.15018(4) | 0.0152(2) |
| S1 | 4e | 0.40059(18) | 0.2618(6) | 0.36632(19) | 0.0114(6) |
| O11 | 4e | 0.2911(5) | 0.2368(12) | 0.3661(5) | 0.0232(19) |
| O12 | 4e | 0.4345(6) | 0.2907(12) | 0.2649(6) | 0.018(2) |
| O13 | 4e | 0.4365(9) | 0.4226(13) | 0.4302(8) | 0.015(3) |
| O14 | 4e | 0.4552(8) | 0.1000(13) | 0.4128(8) | 0.016(2) |
| S2 | 4e | 0.3617(3) | 0.1106(5) | 0.0434(3) | 0.0154(8) |
| O21 | 4e | 0.3497(7) | 0.0131(12) | 0.9480(7) | 0.024(2) |
| O22 | 4e | 0.2609(6) | 0.1648(11) | 0.0780(6) | 0.019(2) |
| O23 | 4e | 0.4216(7) | 0.9994(12) | 0.1174(7) | 0.021(2) |
| O24 | 4e | 0.4243(6) | 0.2766(18) | 0.0275(6) | 0.022(2) |
| S3 | 4e | 0.3468(2) | 0.1063(5) | 0.6518(2) | 0.0139(8) |
| O31 | 4e | 0.3885(8) | 0.0071(12) | 0.7388(7) | 0.024(2) |
| O32 | 4e | 0.8221(7) | 0.5233(13) | 0.0699(7) | 0.020(2) |
| O33 | 4e | 0.2550(6) | 0.2060(12) | 0.6786(6) | 0.022(2) |
| O34 | 4e | 0.4241(6) | 0.2430(17) | 0.6213(5) | 0.0172(18) |
| OW1 | 4e | 0.6433(7) | 0.3930(15) | 0.3676(8) | 0.024(2) |
| OW2 | 4e | 0.6303(8) | 0.3671(14) | 0.9895(8) | 0.027(2) |
| OW3 | 4e | 0.6287(6) | 0.2151(16) | 0.7186(6) | 0.025(3) |
| OW4 | 4e | 0.5503(8) | 0.5764(14) | 0.1642(8) | 0.028(3) |

**Table 5**
Anisotropic displacement parameters $U_{ij}$ ($\text{Å}^2$) for the atoms in $Pr_2(SO_4)_3 \cdot 4H_2O$.

| Atom | $U_{11}$ | $U_{22}$ | $U_{33}$ | $U_{12}$ | $U_{13}$ | $U_{23}$ |
|---|---|---|---|---|---|---|
| Pr1 | 0.0119(4) | 0.0121(4) | 0.0139(4) | −0.0013(5) | 0.0003(3) | −0.0001(5) |
| Pr2 | 0.0129(4) | 0.0151(4) | 0.0177(4) | 0.0032(5) | 0.0010(3) | 0.0000(5) |
| S1 | 0.0107(13) | 0.0122(15) | 0.0112(13) | −0.001(2) | −0.0001(11) | 0.000(2) |
| O11 | 0.014(4) | 0.032(5) | 0.023(4) | −0.001(7) | −0.007(3) | 0.004(6) |
| O12 | 0.020(4) | 0.018(6) | 0.016(4) | 0.000(4) | 0.000(4) | 0.003(4) |
| O13 | 0.025(7) | 0.010(5) | 0.009(6) | −0.008(4) | −0.010(5) | 0.007(5) |
| O14 | 0.015(5) | 0.014(5) | 0.017(6) | −0.002(5) | −0.001(5) | −0.002(4) |
| S2 | 0.0132(18) | 0.0169(19) | 0.0162(19) | 0.0007(16) | 0.0016(16) | 0.0009(16) |
| O21 | 0.026(6) | 0.021(5) | 0.023(5) | −0.008(5) | −0.001(4) | −0.003(4) |
| O22 | 0.007(4) | 0.025(5) | 0.025(5) | −0.013(4) | 0.001(4) | 0.005(4) |
| O23 | 0.015(5) | 0.019(5) | 0.030(5) | −0.002(4) | −0.002(5) | 0.002(4) |
| O24 | 0.021(5) | 0.031(7) | 0.016(4) | 0.002(6) | 0.004(4) | −0.007(6) |
| S3 | 0.0139(18) | 0.0139(18) | 0.0140(18) | 0.0009(16) | 0.0025(15) | 0.0014(15) |
| O31 | 0.032(6) | 0.022(5) | 0.019(5) | 0.004(4) | 0.005(5) | 0.000(5) |
| O32 | 0.011(5) | 0.033(6) | 0.015(5) | 0.005(4) | −0.012(5) | −0.005(4) |
| O33 | 0.013(4) | 0.028(6) | 0.025(5) | −0.006(4) | 0.012(4) | 0.007(4) |
| O34 | 0.020(4) | 0.014(4) | 0.018(4) | 0.002(6) | 0.005(4) | −0.001(7) |
| OW1 | 0.011(5) | 0.033(6) | 0.030(6) | 0.012(5) | 0.001(5) | −0.009(5) |
| OW2 | 0.028(6) | 0.026(6) | 0.029(6) | 0.011(5) | 0.005(5) | −0.010(6) |
| OW3 | 0.008(4) | 0.048(8) | 0.017(4) | 0.008(5) | −0.005(4) | −0.019(5) |
| OW4 | 0.038(7) | 0.018(6) | 0.029(6) | 0.000(5) | 0.005(5) | 0.002(5) |

**Table 6**
Hydrogen bonds in $Ho_2(SO_4)_3 \cdot 8H_2O$.

| D–H | A | d(D–H) (Å) | d(H–A) (Å) | Angle (DHA) (deg) | d(D–A) (Å) |
|---|---|---|---|---|---|
| OW1–H11 | OW2 | 0.72(3) | 2.25 | 167 | 2.95 |
| OW1–H11 | O14 | 0.72(3) | 2.63 | 118 | 3.03 |
| OW1–H12 | O12 | 0.72(3) | 2.18 | 147 | 2.79 |
| OW1–H12 | O13 | 0.72(3) | 2.56 | 128 | 3.04 |
| OW1–H12 | S1 | 0.72(3) | 2.85 | 116 | 3.22 |
| OW2–H21 | O12 | 0.72(3) | 2.38 | 158 | 3.04 |
| OW2–H22 | O22 | 0.72(3) | 2.07 | 171 | 2.76 |
| OW2–H22 | O21 | 0.72(3) | 2.55 | 113 | 2.90 |
| OW2–H22 | S2 | 0.72(3) | 2.78 | 144 | 3.37 |
| OW3–H31 | O11 | 0.72(3) | 2.06 | 174 | 2.75 |
| OW3–H32 | O22 | 0.72(3) | 2.16 | 155 | 2.81 |
| OW4–H41 | O22 | 0.72(3) | 2.13 | 176 | 2.83 |
| OW4–H42 | O11 | 0.72(3) | 2.05 | 163 | 2.73 |

**Table 7**
Hydrogen bonds in $Pr_2(SO_4)_3 \cdot 4H_2O$.

| D–H | A | d(D–H) (Å) | d(H–A) (Å) | Angle (DHA) (deg) | d(D–A) (Å) |
|---|---|---|---|---|---|
| OW1–H11 | O21 | 0.82(5) | 2.23 | 145 | 2.93 |
| OW1–H12 | O13 | 0.82(5) | 2.45 | 110 | 2.87 |
| OW2–H21 | O11 | 0.82(5) | 2.09 | 150 | 2.83 |
| OW2–H22 | O21 | 0.82(5) | 2.14 | 148 | 2.87 |
| OW2–H22 | O23 | 0.82(5) | 2.39 | 140 | 3.06 |
| OW2–H22 | S2 | 0.82(5) | 2.66 | 171 | 3.47 |
| OW3–H31 | O11 | 0.82(5) | 2.24 | 132 | 2.85 |
| OW3–H31 | O22 | 0.82(5) | 2.33 | 112 | 2.75 |
| OW3–H32 | O11 | 0.82(5) | 2.18 | 140 | 2.85 |
| OW4–H41 | OW3 | 0.82(5) | 2.42 | 175 | 3.24 |
| OW4–H42 | O24 | 0.82(5) | 1.99 | 168 | 2.80 |
| OW4–H42 | OW2 | 0.82(5) | 2.64 | 116 | 3.08 |

**Table 8**
Selected interatomic distances (Å) and angles (deg) in $Ho_2(SO_4)_3 \cdot 8H_2O$, $Tm_2(SO_4)_3 \cdot 8H_2O$, and $Pr_2(SO_4)_3 \cdot 4H_2O$.

| | $Ho_2(SO_4)_3 \cdot 8H_2O$ | $Tm_2(SO_4)_3 \cdot 8H_2O$ | $Pr_2(SO_4)_3 \cdot 4H_2O$ |
|---|---|---|---|
| $Ln$–O | 2.281(4)–2.459(4) | 2.258(4)–2.439(4) | 2.335(9)–2.690(10) |
| S–O | 1.450(4)–1.491(4) | 1.451(4)–1.489(4) | 1.440(8)–1.500(10) |
| O–$Ln$–O | 79.91(14)–144.17(12) | 68.63(12)–147.25(15) | 53.5(2)–150.0(3) |
| O–S–O | 107.4(2)–111.9(2) | 107.9(2)–111.9(2) | 104.9(5)–113.2(6) |

form eight-membered moieties connected via hydrogen bonds (Fig. S1), the relative arrangement of these is shown in Figs. S2 and S3 (Supplementary Material).
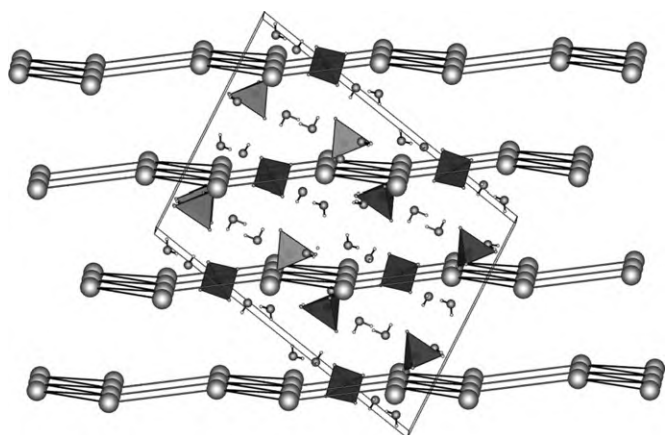
Fig. 1. Representation of the crystal structure of $Ln_2(SO_4)_3 \cdot 8H_2O$ ($Ln$=Ho, Tm) viewed along the $b$-axis. Light grey indicates $Ln$ cations which form slightly undulated layers. Between the layers $SO_4$ tetrahedra (dark grey) and water molecules are positioned.
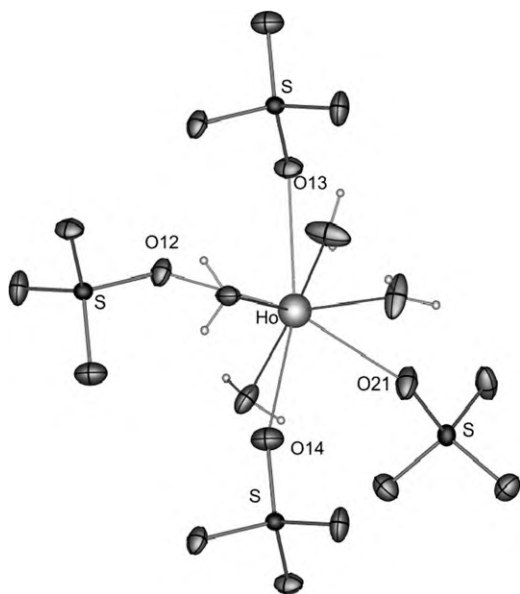


Fig. 2. Coordination environments of Ho. The displacement ellipsoids are drawn at a 50% probability level.

## 4. Crystal structure of $Pr_2(SO_4)_3 \cdot 4H_2O$

$Pr_2(SO_4)_3 \cdot 4H_2O$ crystallises isotypically with $Ln_2(SO_4)_3 \cdot 4H_2O$ (La, Nd [1], Ce [2]) but it is not isostructural to $Er_2(SO_4)_3 \cdot 4H_2O$, which adopts space group $P-1$ (no. 2) [3]. Rather frequently, the compounds of the heavier and smaller rare-earth ions adopt different crystal structures as the larger ones [20]. The asymmetric unit of the unit cell consists of two crystallographically different Pr atoms, three sulphate tetrahedra and four crystal water molecules. The praseodymium atoms form two different zigzag chains running along [010] which are interconnected to form undulated layers with the sulphate tetrahedra and crystal water molecules in the voids of the resulting structure (Fig. 3). The Pr1–Pr1 distances amount to 4.212 and 4.437 Å, while the Pr2–Pr2 distances are 5.537 and 5.779 Å. The coordination spheres of the praseodymium atoms are shown in Fig. 4. Pr1 is surrounded by nine (two $H_2O$ and seven monodentate sulphate groups) and Pr2 by eight oxygen atoms (two $H_2O$, six sulphate groups) forming irregular [$Pr1O_9$] polyhedra and square

antiprisms [$Pr2O_8$]. The Pr–O bond lengths vary from 2.335(9) to 2.690(10) Å. The S–O distances within the tetrahedral anions vary in a range from 1.440(8) to 1.500(10) Å and the O–S–O angles range between 104.9° and 113.2°.

The water molecules donate hydrogen atoms that form hydrogen bond networks of moderate strength [18,19] with sulphate and water O atoms with $d$(OW–O)=2.797–3.472 Å, respectively. The crystal water molecules form a hydrogen bond network of two-dimensionally knotted strings as shown in Fig. S4, the relative arrangement of these sheets is shown in Fig. S5 (Supplementary Material).

## 5. Vibrational spectroscopy of $Ho_2(SO_4)_3 \cdot 8H_2O$ and $Pr_2(SO_4)_3 \cdot 4H_2O$

Fig. 5 presents the IR and Raman spectra of $Ho_2(SO_4)_3 \cdot 8H_2O$ (**a**) and $Pr_2(SO_4)_3 \cdot 4H_2O$ (**b**). The infrared spectra of both sulphates are similar. The absorption band from 3480 to 2900 $cm^{-1}$ can be assigned to O–H stretching vibrations ($\nu$(OH)) of water molecules affected by hydrogen bonding. At 1640 (**a**) $cm^{-1}$ and 1720 $cm^{-1}$ (**b**) weak bands are observed, attributable to the bending modes ($\sigma$(OH)) of the crystal water molecules. The characteristic frequencies of the normal vibration modes of a free tetrahedral $SO_4^{2-}$ ion are found between 1290 and 400 $cm^{-1}$ [21]. Strong peaks are observed around 1100 $cm^{-1}$ for **a** and very weak peaks at 1070 $cm^{-1}$ for **b** which were assigned to $\nu_{as}(SO_4)$ stretching frequencies. The vibrations excited around 1000 $cm^{-1}$ for $Ho_2(SO_4)_3 \cdot 8H_2O$ and 890 $cm^{-1}$ for $Pr_2(SO_4)_3 \cdot 4H_2O$ bands could be assigned to the total symmetric stretching vibration ($\nu_s$) of the $SO_4^{2-}$ anion [22]. For $Pr_2(SO_4)_3 \cdot 4H_2O$ this peak is found to be shifted to lower wave numbers than normally observed for isolated sulphate groups. This can be explained by the present strong hydrogen bonds weakening the SO bond [23,24]. The intense sharp band from 610 to 560 $cm^{-1}$ can be ascribed to the $\delta_{as}(SO_4)$ vibration, and the peaks observed at 430 $cm^{-1}$ (**a**) and 460 $cm^{-1}$ (**b**) are assigned to symmetric bending modes.

In the Raman spectra of $Ho_2(SO_4)_3 \cdot 8H_2O$ and $Pr_2(SO_4)_3 \cdot 4H_2O$, asymmetric stretching mode of the $SO_4^{2-}$ is detected at 1240 $cm^{-1}$. At 1017 $cm^{-1}$ (**a**) and 1040 $cm^{-1}$ (**b**) a very intense band of a symmetric stretching mode is observed. Similarly, the respective Raman bands in the region appear around 600 $cm^{-1}$ (asymmetric bending vibration) while the band peaking at 468 $cm^{-1}$ represents the symmetric bending vibration of $SO_4^{2-}$ ion. The observed frequencies in the spectra correspond very well with the expected values.

## 6. UV–vis spectroscopy of $Ho_2(SO_4)_3 \cdot 8H_2O$ and $Pr_2(SO_4)_3 \cdot 4H_2O$

The UV–vis spectra of $Ho_2(SO_4)_3 \cdot 8H_2O$ and $Pr_2(SO_4)_3 \cdot 4H_2O$ are shown in Figs. 6 and 7. Therein all relevant 4$f$–4$f$ transitions are indicated according to the well known energy level schemes of both lanthanide ions [25]. In $Ho_2(SO_4)_3 \cdot 8H_2O$ all transitions start from the ground state $^5I_8$, in $Pr_2(SO_4)_3 \cdot 4H_2O$ from the ground state $^3H_4$. No significant deviations from the spectra of other inorganic salts of Ho and Pr were detected and the spectra are in accordance with the crystal colours green (Pr compound) and pink/yellow (Ho). $Ho_2(SO_4)_3 \cdot 8H_2O$ shows an Alexandrite effect, a colour change upon irradiation with different light sources [26,27]; it looks pink under light emission of luminescent tubes due to the absorption in the green wavelength range around 540 nm and yellow under ambient day light, when the bluish part (bands around 400 and 450 nm) of the black body radiation emitted by the sun is absorbed.
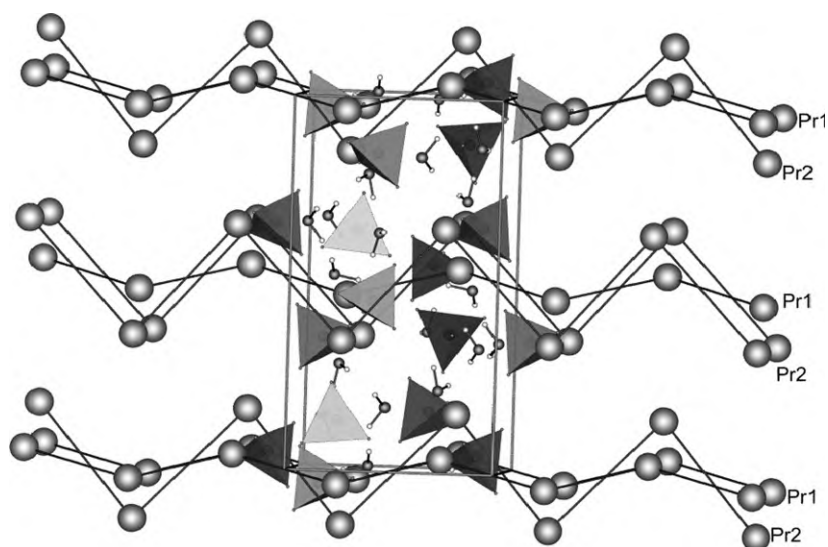
**Fig. 3.** The unit cell of the crystal structure of $Pr_2(SO_4)_3 \cdot 4H_2O$ viewed along the *a*-axis. Grey spheres represent the Pr atoms, the sulphate tetrahedra are drawn as semitransparent light grey polyhedra.



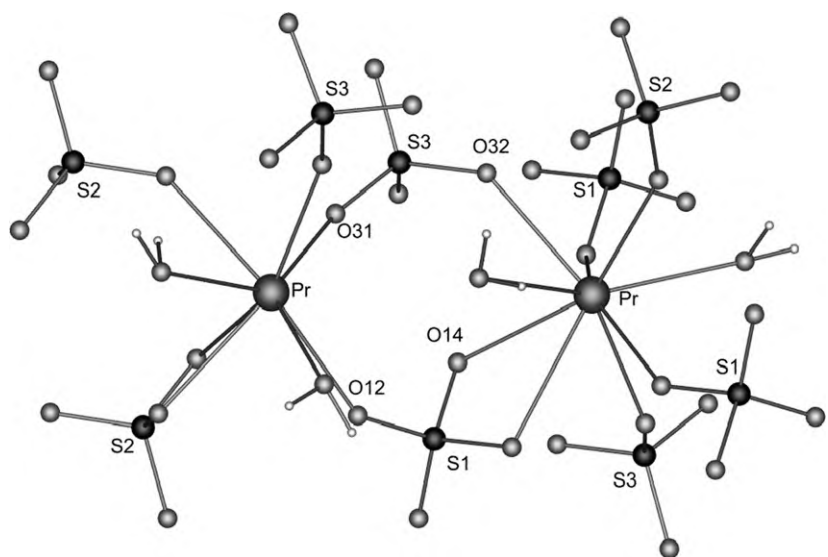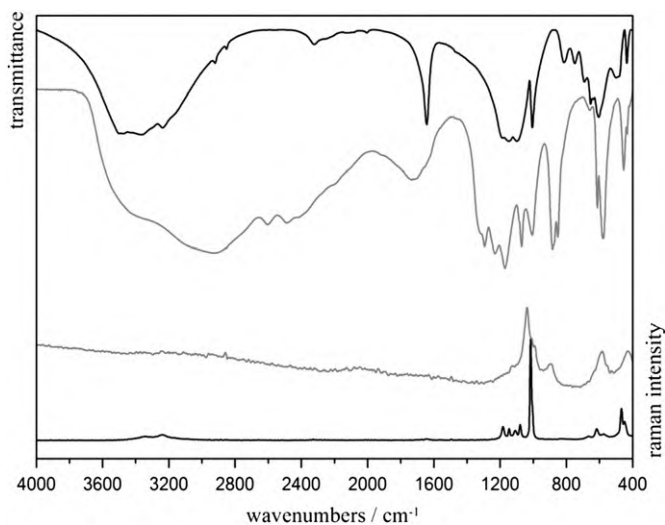**Fig. 4.** Coordination environments of Pr1 and Pr2.



**Fig. 5.** Vibrational spectra of $Ho_2(SO_4)_3 \cdot 8H_2O$ (black) and $Pr_2(SO_4)_3 \cdot 4H_2O$ (grey).
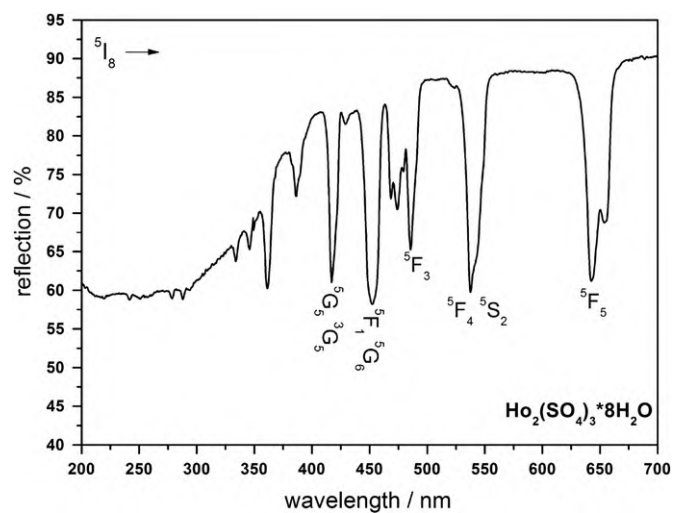


**Fig. 6.** UV–vis reflection spectrum of $Ho_2(SO_4)_3 \cdot 8H_2O$; all relevant transitions have been indicated.

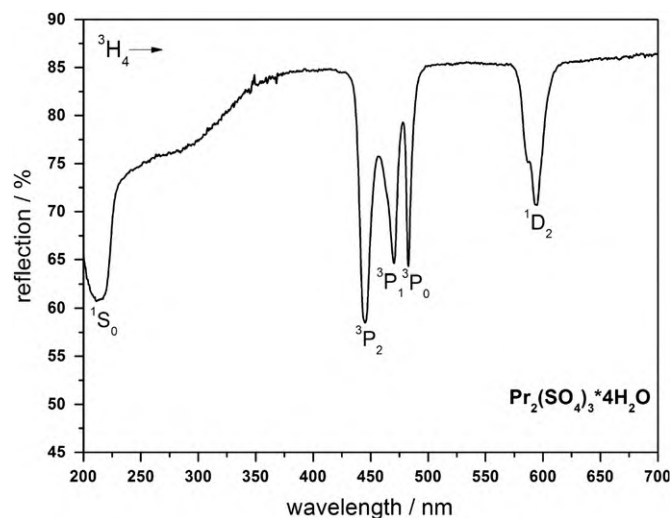**Fig. 7.** UV–vis reflection spectrum of $Pr_2(SO_4)_3 \cdot 4H_2O$; all relevant transitions have been indicated.

## 7. Discussion and conclusions

In this contribution we presented the crystal structures of $Ln_2(SO_4)_3 \cdot 8H_2O$ ($Ln$=Ho, Tm) and $Pr_2(SO_4)_3 \cdot 4H_2O$. Thus all crystal structures of the lanthanide octahydrates are clarified now, all of them are isotypic and adopt space group $C2/c$. Both structure types, the octahydrates and the tetrahydrates, exhibit basically a layered arrangement of the cations with the sulphate ions in-between. Very different are the arrangements of the crystal water molecules forming the hydrogen bond networks in the two structure types of $Ho_2(SO_4)_3 \cdot 8H_2O$ and $Pr_2(SO_4)_3 \cdot 4H_2O$. Surprisingly, in the holmium compound containing more crystal water relatively small moieties without direct contact to others are formed while in the praseodymium compound containing less crystal water an extended network is formed.

The vibrational spectra are in accordance with the structure models, and the optical properties of the lanthanide compounds comprise the normal absorptions due to $4f$–$4f$ transitions which are not significantly affected by crystal field effects.

## Appendix A. Supporting data

Supplementary data associated with this article can be found in the online version at doi:10.1016/j.jssc.2011.03.024.

## References

[1] S. Bade, Jiegon Huaxue 6 (1987) 70.
[2] B.M. Casari, V. Langer, Z. Anorg. Allg. Chem. 633 (2007) 1074.
[3] D.Y. Wei, Y.-Q. Zheng, Z. Kristallogr. 218 (2003) 23.
[4] P. Held, M.S. Wickleder, Acta Crystallogr. E59 (2003) i98.
[5] P.C. Junk, C.J. Kepert, B.W. Skelton, A.H. White, Aust. J. Chem. 52 (1999) 601.
[6] S. Ahmed Farag, M.A. El Kordy, N.A. Ahmed, Z. Kristallogr. 155 (1981) 161.
[7] H. Bartl, E. Rodek, Z. Kristallogr. 162 (1983) 13.
[8] N.V. Podberezskaya, S.V. Borisov, Zh. Struk. Khim. 17 (1976) 186.
[9] T.R. Sarangarajan, K. Panchanatheswaran, J.N. Low, C. Glidewell, Acta Crystallogr. E60 (2004) i142.
[10] H.U. Hummel, E. Fischer, T. Fischer, P. Joerg, G. Pezzei, Z. Anorg. Allg. Chem. 619 (1993) 805.
[11] M.S. Wickleder, Z. Anorg. Allg. Chem. 625 (1999) 1548.
[12] L. Hiltunen, L. Niinisto, Cryst. Struct. Commun. 6 (1976) 561.
[13] C. Cascales, B.G. Lor, E. Gutiérrez, M.Iglesias Puebla, M.A. Monge, C. Ruíz Valero, N. Snejko, Chem. Mater. 16 (2004) 4144.
[14] K. Kazmierczak, H.A. Höppe, J. Solid State Chem. 183 (2010) 2087.
[15] Stoe & Cie (Darmstadt), Programs X-Red and X-SHAPE, 1999.
[16] SADABS: Area-Detector Absorption Correction. Siemens Industrial Automation Inc., Madison, WI, 1996.
[17] G.M. Sheldrick, SHELXTL, V.5.10 Crystallographic System, Bruker AXS Analytical X-ray Instruments Inc., Madison, 1997.
[18] G.A. Jeffrey, An Introduction to Hydrogen Bonding, Oxford University Press, Oxford, 1997.
[19] T. Steiner, Angew. Chem. Int. Ed. 41 (2002) 48.
[20] H.A. Höppe, S.J. Sedlmaier, Inorg. Chem. 46 (2007) 3467.
[21] J.T. Kloprogge, H. Ruan, L.V. Duong, R.L. Frost, Neth. J. Geosci. 80 (2001) 41.
[22] J. Baran, M.M. Ilczyszyn, M.K. Marchewka, H. Ratajczak, Spectrosc. Lett. 32 (1) (1999) 83.
[23] J. Weidlein, U. Müller, K. Dehnicke, Schwingungsspektroskopie, Georg Thieme Verlag, Stuttgart, New York, 1988.
[24] J. Weidlein, U. Müller, K. Dehnicke, Schwingungsfrequenzen I, Hauptgruppenelemente, Georg Thieme Verlag, Stuttgart, New York, 1981.
[25] G.H. Dieke, Spectra and Energy Levels of Rare Earth Ions in Crystals, John Wiley & Sons, London, 1968.
[26] H.A. Höppe, G. Kotzyba, R. Pöttgen, W. Schnick, J. Mater. Chem. 11 (2001) 3300.
[27] S.S. Matsyuk, A.N. Platonov, M.N. Taran, G.I. Smirnov, A.S. Povarennykh, Dopov. Akad. Nauk Ukr. RSR B 1 (1980) 27.